

Synthesis, Microwave Spectrum, and Conformational Equilibrium of Propa-1,2-dienethiol ($\text{H}_2\text{C}=\text{C}=\text{CHSH}$)

Harald Møllendal,^{*,†} Brahim Khater,^{‡,§} and Jean-Claude Guillemin^{*,‡,§}

Centre for Theoretical and Computational Chemistry (CTCC), Department of Chemistry, University of Oslo, P.O. Box 1033 Blindern, NO-0315 Oslo, Norway, École Nationale Supérieure de Chimie de Rennes, CNRS, UMR 6226, Avenue du Général Leclerc, CS 50837, 35708 Rennes Cedex 7, France, and Université Européenne de Bretagne, 35000 Rennes, France

Received: February 27, 2009; Revised Manuscript Received: March 31, 2009

The first synthesis of the kinetically unstable compound propa-1,2-dienethiol (allenethiol; $\text{H}_2\text{C}=\text{C}=\text{CHSH}$) is reported. Its microwave spectrum has been studied in the 41.5–80 GHz spectral range. The spectra of two rotameric forms have been assigned. The C–C–S–H chain of atoms is *synperiplanar* (0°) in one of the conformers. This dihedral angle is *anticlinal* in the second rotamer forming an angle of $140(5)^\circ$ in the second form. The *synperiplanar* conformer is found to be 1.0(6) kJ/mol more stable than the *anticlinal* rotamer. The microwave study has been augmented by quantum chemical calculations at the MP2/aug-cc-pVTZ and B3LYP/6-311++G** levels of theory. The predictions of these two theoretical methods are in excellent agreement with the experimental findings.

Introduction

Many years ago, the microwave (MW) spectra of two rotameric forms of ethenethiol ($\text{H}_2\text{C}=\text{CHSH}$) were reported.^{1,2} One of these rotamers has a *synperiplanar* (obsolete: “cis”) arrangement for the C–C–S–H chain of atoms,¹ whereas this link is effectively *antiperiplanar* in the other conformer.² A study of vibrationally excited states of the *antiperiplanar* form revealed the presence of a small potential barrier of 19 cm^{-1} (0.23 kJ/mol) at the exact planar conformation.² The ground vibrational state was found to lie above the top of the barrier.² It was also found that the *synperiplanar* form is more stable than the *antiperiplanar* rotamer by 0.6(3) kJ/mol.²

The corresponding methyl thioether, methyl vinyl sulfide ($\text{H}_2\text{C}=\text{CHSCH}_3$), also prefers a C–C–S–C *synperiplanar* conformer, which is 5.0(3) kJ/mol more stable than an *anticlinal* form, where this dihedral angle is approximately 154° .³ The substitution of hydrogen atom of the thiol group in ethenethiol with a methyl group is therefore seen to have a large effect on the conformational composition.

Interaction between neighboring groups is often decisive for the conformational properties of a compound. Propa-1,2-dienethiol, allenethiol, ($\text{H}_2\text{C}=\text{C}=\text{CHSH}$) differs from ethenethiol ($\text{H}_2\text{C}=\text{CHSH}$) in that the vinyl ($\text{H}_2\text{C}=\text{CH}$) group has been replaced by the somewhat similar allenyl group ($\text{H}_2\text{C}=\text{C}=\text{CH}$). The object of the present work has been to see what structural and conformational consequences this change results in.

The title compound has not previously been available presumably because the synthesis of this compound, as well as of other propa-1,2-dienyl heterocompounds of group 14 – 16 of the Periodic Table bearing one or more hydrogen atoms on the heteroatom, are difficult.^{4–11} Recently, the structural and conformational properties of two such compounds, namely,

$\text{H}_2\text{C}=\text{C}=\text{CHGeH}_3$ and $\text{H}_2\text{C}=\text{C}=\text{CHSnH}_3$, have been investigated by electron diffraction.⁴ A MW study of the corresponding phosphine, $\text{H}_2\text{C}=\text{C}=\text{CHPH}_2$, has also been reported.¹² The simple compound allenylsilane, $\text{H}_2\text{C}=\text{C}=\text{CHSiH}_3$, has so far not been synthesized.

The present study also represents an extension of our recent investigations of the conformational properties of thiols such as 3-butyne-1-thiol ($\text{HSCH}_2\text{CH}_2\text{C}\equiv\text{CH}$),¹³ (Z)-3-mercapto-2-propenenitrile ($\text{HSCH}=\text{CHCN}$),¹⁴ cyclopropanethiol ($\text{C}_3\text{H}_5\text{SH}$),¹⁵ and 2,2,2-trifluoroethanethiol $\text{CF}_3\text{CH}_2\text{SH}$,¹⁶ using MW spectroscopy augmented with quantum chemical calculations.

MW spectroscopy was chosen for this study because of the extremely high accuracy and resolution of this method, making it especially suitable for conformational studies. The spectroscopic work has been augmented by high-level quantum chemical calculations, which were conducted with the purpose of obtaining information for the use in assigning the MW spectra and investigating properties of the potential-energy hypersurface.

Experimental Section

Synthesis of Propa-1,2-dienethiol (Allenethiol). *Caution!* Propa-1,2-dienethiol is malodorous and potentially toxic. All reactions and handling should be carried out in a well-ventilated hood.

Propa-1,2-dienethiol has been prepared by a chemoselective reduction of the corresponding thiocyanate. The latter has been synthesized as previously reported.¹⁷

LiAlH_4 (0.1 g, 2.4 mmol) and dry tetraglyme (20 mL) were introduced into a 50 mL two-necked flask equipped with a stirring bar and a nitrogen inlet. The flask was immersed in a cold bath (-30°C), and aluminum chloride (1.0 g, 7.5 mmol) was added in portions. The reaction mixture was allowed to warm to -10°C and stirred for 5 min. Propa-1,2-dienylthiocyanate (291 mg, 3.0 mmol) diluted in dry tetraglyme (10 mL) was then added dropwise for about 5 min and the mixture was stirred for 5 min at -10°C . Succinic acid (4.72 g, 40 mmol) and tetraglyme (20 mL) were introduced into a 100 mL two-necked round-bottomed flask equipped with a stirring bar and

* To whom correspondence should be addressed. Telephone: +47 2285 5674. Fax: +47 2285 5441. E-mail: (H.M.) harald.mollendal@kjemi.uio.no; (J.-C.G.) jean-claude.guillemin@ensc-rennes.fr.

[†] University of Oslo.

[‡] École Nationale Supérieure de Chimie de Rennes.

[§] Université Européenne de Bretagne.

a septum. The flask was attached to a vacuum line equipped with two cells, degassed, and then immersed in a cold bath ($-10\text{ }^{\circ}\text{C}$). The mixture containing aluminum thiolate was slowly added with a syringe through the septum into the flask containing the succinic acid. During and after the addition, propadiene-1,2-thiol was distilled off in vacuo (10^{-1} mbar) from the reaction mixture. The first trap cooled at $-60\text{ }^{\circ}\text{C}$ removed selectively the less volatile products, and allenethiol was selectively condensed in the second trap equipped with two stopcocks and cooled at $-110\text{ }^{\circ}\text{C}$. About 15 min after the end of the addition, the stopcocks were closed to avoid the trapping of a byproduct more slowly formed, namely, hydrogen cyanide. The second cell was disconnected from the vacuum line by stopcocks and adapted to the MW spectrometer.

To record the NMR spectra, this second trap was allowed to warm to room temperature and the products were condensed on a coldfinger ($-196\text{ }^{\circ}\text{C}$) connected at the bottom to an NMR tube immersed in liquid nitrogen. A cosolvent (CDCl₃) was added at this step. After disconnection from the vacuum line by stopcocks, the apparatus was filled with dry nitrogen; liquid nitrogen was subsequently removed. The products were collected in the NMR tube and kept at low temperature ($<-50\text{ }^{\circ}\text{C}$) before analysis. Yield: 119 mg, 1.65 mmol, 55%, bp $\approx -70\text{ }^{\circ}\text{C}$ (0.1 mbar). $\tau_{1/2}$ (5% in CDCl₃ at room temperature): 30 h. ¹H NMR (400 MHz, CDCl₃): δ 2.62 (dt, 1H, $^3J_{\text{HH}} = 7.6\text{ Hz}$, $^5J_{\text{HH}} = 2.0\text{ Hz}$, SH); 4.94 (dd, 2H, $^4J_{\text{HH}} = 6.6\text{ Hz}$, $^5J_{\text{HH}} = 2.0\text{ Hz}$, CH₂); 5.66 (td, 1H, $^4J_{\text{HH}} = 7.6\text{ Hz}$, $^3J_{\text{HH}} = 6.6\text{ Hz}$, CH-S). ¹³C NMR (100 MHz, CDCl₃): δ 78.3 (d, $^1J_{\text{CH}} = 191.1\text{ Hz}$, CH); 78.9 (t, $^1J_{\text{CH}} = 169.5\text{ Hz}$, CH₂); 208.0 (s, C=C=C). IR (ν , cm⁻¹, gas phase, 20 $^{\circ}\text{C}$): 3050 (m, $\nu_{\text{C}=\text{CH}_2}$), 2967 (s), 2886 (m), 2597 (w, ν_{SH}), 1954 (m, $\nu_{\text{C}=\text{C}=\text{C}}$), 1259 (s), 1135 (m), 852 (s). HRMS: calcd for C₃H₄³²S, 72.0034; found, 72.003.

Microwave Experiment. The MW spectrum was recorded in the 41.5–80 GHz spectral region, using the Stark-modulated spectrometer of the University of Oslo. Details of the construction and operation of this spectrometer, which has a 2 m Hewlett-Packard Stark cell, have been given elsewhere.^{18,19} The spectrum was taken with the cell cooled to roughly $-30\text{ }^{\circ}\text{C}$. The spectral lines were measured with an estimated accuracy of $\approx \pm 0.15\text{ MHz}$ for isolated lines. Radio frequency microwave double resonance experiments (RFMWDR), similar to those performed by Wodarczyk and Wilson,²⁰ were also conducted to assign unambiguously particular transitions. Allenethiol is kinetically unstable and precautions were taken to avoid undesirable products to be formed in the samples during the MW study, which took several weeks to perform. In this period, the samples were kept at dry ice temperature ($-78\text{ }^{\circ}\text{C}$), or at liquid-nitrogen temperature ($-196\text{ }^{\circ}\text{C}$) when not in use. In spite of this, numerous strong MW lines not belonging to the title compound were observed and identified in some cases, indicating the presence of considerable amounts of impurities. Attempts to remove the impurities by pumping on the sample held at dry ice temperature met with some success, but the impurities were never completely removed and rendered the spectrum significantly less intense than it would have been with a pure sample.

Results

Quantum Chemical Calculations. The present *ab initio* and density functional theory (DFT) calculations were performed employing the Gaussian 03 suite of programs,²¹ running on the Titan cluster in Oslo. Electron correlation was taken into consideration in the *ab initio* calculations using Møller–Plesset second-order perturbation calculations (MP2),²² Becke's three-parameter hybrid functional²³ employing the Lee, Yang and Parr

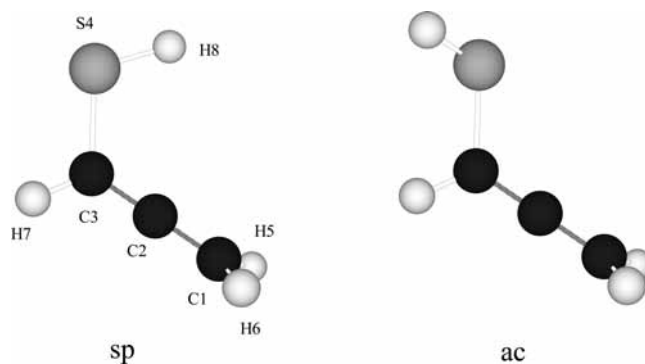


Figure 1. The *synperiplanar* (**sp**) and *anticlinal* (**ac**) rotamers of H₂C=C=CHSH. Atom numbering is shown on **sp**. The microwave spectra of both these conformers were assigned. **sp** was found to be 1.0(6) kJ/mol more stable than **ac**.

correlation functional (B3LYP)²⁴ was employed in the DFT calculations. Peterson and Dunning's²⁵ correlation-consistent triple- ζ wave function augmented with diffuse functions, aug-cc-pVTZ, were used in the MP2 calculations, whereas the 6-311++G** basis set was employed in the DFT calculations.

A model of this compound with atom numbering is shown in Figure 1. Rotation about the C3–S4 bond may produce rotational isomerism. MP2 calculations were performed in an attempt to predict which rotameric forms that are minima (“stable”) of the potential-energy hypersurface. Calculations of energies were performed for the 0 (*synperiplanar*) to 180° (*antiperiplanar*) interval in steps of 10° of the C–C–S–H dihedral angle, employing the scan option of the Gaussian 03 program, allowing all remaining structural parameters to vary freely. The resulting potential function has two minima at 0 (*synperiplanar*) and about 140° (*anticlinal*) of the C–C–S–H dihedral angle, and maxima at approximately 70 and 180°. The two “stable” conformers at 0 and 140° predicted in these calculations are henceforth denoted **sp** and **ac** and they are sketched in Figure 1, where the atom numbering is also indicated.

The two maxima of the potential function were explored next using the transition-state option of Gaussian 03. The first maximum was found at 68.9° (from *synperiplanar*) of the C2–C3–S4–H8 dihedral angle with an electronic energy that is 6.30 kJ/mol higher than the energy of the global minimum **sp**. The second maximum was found at exactly 180° (*antiperiplanar*), 2.97 kJ/mol above the energy of **sp**. Each of these maxima has one imaginary vibrational frequency associated with the torsion about the C3–S4 bond, which indicates that they are first-order transition states. Interestingly, the predicted barrier at 180° (*antiperiplanar*) of 2.97 kJ/mol is roughly 10 times larger than the corresponding experimental barrier (0.23 kJ/mol) in H₂C=C=CHSH.²

Separate MP2 calculations of the structures, energies, dipole moments, vibrational frequencies, and Watson's quartic *A*-reduction centrifugal distortion constants²⁶ were undertaken next. The starting values of the C2–C3–S4–H8 dihedral angles were chosen to be close to 0 and 140°, respectively. Full geometry optimizations with no symmetry restrictions were made employing the default convergence criteria of Gaussian 03. The C2–C3–S4–H8 dihedral angle was found to be exactly 0° in **sp**, which is therefore predicted to have a symmetry plane (*C_s* symmetry). This angle was calculated to be 140.3° in **ac**. Only positive values were found for the vibrational frequencies of each of the two conformers, which indicates that they are minima on the energy hypersurface. The MP2 structures of **sp**

TABLE 1: MP2/aug-cc-pVTZ Structures of the Synperiplanar and Anticlinical Conformers of H₂C=C=CHSH

conformer	bond distance (pm)	
	sp	ac
C1–C2	131.1	130.9
C1–H5	108.3	108.2
C1–H6	108.3	108.2
C2–C3	130.8	131.0
C3–S4	177.1	177.6
C3–H7	108.3	108.2
S4–H8	133.8	133.9

conformer	angle (deg)	
	sp	ac
C2–C1–H5	121.0	120.9
C2–C1–H6	121.0	120.8
H5–C1–H6	118.0	118.3
C2–C3–S4	125.7	121.4
C2–C3–H7	120.9	120.7
S4–C3–H7	113.4	117.6
C3–S4–H8	95.8	96.1
C1–C2–C3	179.0	179.2

conformer	dihedral angle (deg)	
	sp	ac
H5–C1–C3–S4	–90.0	–84.4
H5–C1–C3–H7	90.0	89.4
H6–C1–C3–S4	90.0	95.4
H6–C1–C3–H7	–90.0	–90.8
C2–C3–S4–H8	0.0	–140.3
H7–C3–S4–H8	–180.0	45.2

TABLE 2: MP2 Parameters^a of Spectroscopic Interest of the sp and ac Conformers of H₂C=C=CHSH^b

	sp	ac
Rotational Constants (MHz)		
<i>A</i>	30017.1	29151.9
<i>B</i>	2813.5	2838.2
<i>C</i>	2618.7	2651.8
Quartic Centrifugal Distortion Constant (kHz) ^b		
Δ_J	1.07	1.19
Δ_{JK}	–58.1	–60.4
Δ_K	1381	1377
δ_J	0.195	0.198
δ_K	5.54	6.93
Dipole Moment ^c (10 ^{–30} C m)		
μ_a	3.97	2.39
μ_b	0.95	3.18
μ_c	0.0 ^d	1.48
Δ^e (10 ^{–20} MHz u m ²)		
	–3.48	–4.82
Energy Difference ^f (kJ/mol)		
	0.0	1.49

^a Basis set: aug-cc-pVTZ. ^b For the ³²S isotopologue. ^c $D = 3.33564 \times 10^{-30}$ C m. ^d For symmetry reasons. ^e $\Delta = I_c - I_b - I_a$, where I_a , I_b , and I_c are the principal moments of inertia. Conversion factor: $505379.05 \times 10^{-20}$ MHz u m². ^f Relative to **sp** and corrected for zero-point-vibrational effects. Electronic energy of **sp**: –1349398.9 kJ/mol.

and **ac** are found in Table 1 and parameter of spectroscopic interest are listed in Table 2. The full electronic potential function for rotation about the C3–S4 bond, which could now be drawn, is shown in Figure 2.

The electronic energy difference between the two rotamers was predicted to be 1.84 kJ/mol, with **sp** as the more stable

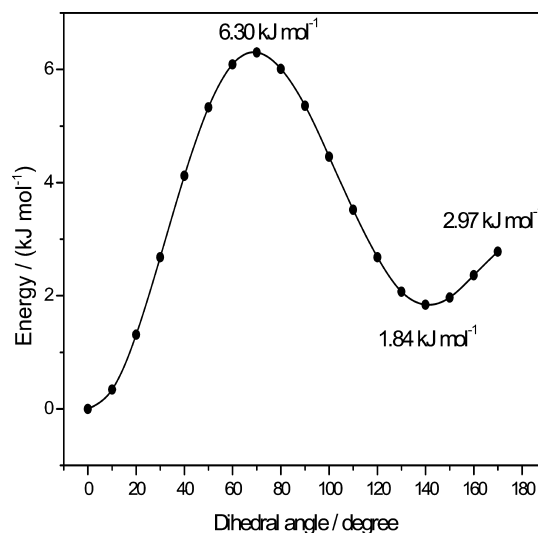


Figure 2. MP2/aug-cc-pVTZ electronic potential function for rotation about the C3–S4 bond in H₂C=C=CHSH. The values of the C2–C3–S4–H8 dihedral angle in degree are given on the abscissa and the relative energies in kJ/mol are given on the ordinate. **sp** has a C2–C3–S4–H8 dihedral angle of exactly 0°. A dihedral angle of 140.3° is predicted for **ac**, which is calculated to be 1.84 kJ/mol less stable than the global minimum, **sp**. This potential function has maxima at 68.9° (6.30 kJ/mol above the energy of **sp**), and at exactly 180° (2.97 kJ/mol above the energy of **sp**).

form. This energy difference is changed slightly to 1.49 kJ/mol when the effects of the harmonic zero-point vibrational energies are taken into consideration.

The B3LYP/6-311++G** calculations were performed primarily to obtain the vibration–rotation constants (the α 's),²⁷ because MP2/aug-cc-pVTZ calculations of these constants are too expensive for our available computational resources. It should be pointed out that the Watson quartic centrifugal distortion constants²⁶ and the vibration–rotation constants²⁷ reported in this work have been obtained in the default standard-orientation axis system of Gaussian 03, and not in the principal-inertial axis system.²⁸ It is expected that this difference would result in minor variations in these constants.

The same two rotamers (**sp** and **ac**) were predicted to be minima (“stable”) on the potential energy hypersurface in the DFT calculations. The C2–C3–S4–H8 dihedral angle of **sp** was found to be exactly 0°, while this angle was calculated to be 143.2° in **ac**. The B3LYP structures of these two rotamers are given in the Supporting Information, Table 1S, with additional parameters of interest found in Table 2S. The B3LYP energy difference corrected for zero-point vibrational frequency was 1.13 kJ/mol. The differences obtained in the MP2 and B3LYP calculations are rather minor, as can be seen by comparing the results in Tables 1 and 2 with their counterparts in Tables 1S and 2S in the Supporting Information.

Microwave Spectrum and Assignment of sp. The observed MW spectrum was crowded with absorption lines occurring every few MHz. The most intense lines were found to belong to impurities, as already mentioned. The transitions of allenethiol were often blended by stronger impurity lines.

According to the quantum chemical calculations shown in Table 2, the μ_a component of the dipole moment of **sp** is much larger than μ_b . The comparatively strong *R*-branch transitions of the spectrum of **sp** were therefore searched for first, using the spectroscopic constants of Table 2 to predict their approximate frequencies of this nearly prolate asymmetrical top (Ray's asymmetry parameter²⁹ $\kappa \approx -0.99$). These searches were

TABLE 3: Spectroscopic Constants^a of the *sp* Conformer of H₂C=C=CHSH

vibrational state	ground	first excited C–C–SH torsion
<i>A</i> /MHz	30136.7 (47)	30109 ^b
<i>B</i> /MHz	2812.3013 (39)	2814.149 (15)
<i>C</i> /MHz	2617.1262 (42)	2620.671 (14)
Δ_J /kHz	1.085 (7)	1.072 (16)
Δ_{JK} /kHz	−59.049 (20)	−59.761 (43)
Δ_K /kHz	1381 ^b	1381 ^b
δ_J /kHz	0.195 ^b	0.195 ^b
δ_K /kHz	5.54 ^b	5.54 ^b
number of transitions	99	26
rms ^c /MHz	0.129	0.096

^a Key: *A*, reduction; *I*^r, representation.²⁶ Uncertainties represent one standard deviation. ^b Fixed. ^c Root-mean-square deviation.

performed using a relatively low Stark field strength in order to modulate only the high-*K*₁ lines. These transitions were found very close to their predicted frequencies. The fact that they form a characteristic pattern facilitated their assignments.

RFMWDR experiments were then undertaken to assign *K*₁ = 3 lines unambiguously. The lowest *K*₁-transitions were ultimately assigned exploiting their modulation properties and fit to Watson's Hamiltonian.²⁶ The strongest *b*-type lines of this conformer were searched for next, but no assignments could be made presumably because μ_b is too small ($\mu_b \approx 0.95 \times 10^{-30}$ C m; Table 2), resulting in a very weak spectrum. The spectroscopic constants of this rotamer were determined from 99 ^a*R*-transitions in a least-squares fit using Sørensen's program Rotfit.³⁰ It was only possible to determine two of Watson's quartic centrifugal distortion constants,²⁶ namely Δ_J and Δ_{JK} , due to the near-prolacy of this conformer. The remaining quartic constants were preset at the MP2 values (Table 2) in the least-squares fit. The spectroscopic constants are listed in Table 3, whereas the full spectrum is given in the Supporting Information, Table 3S.

Comparison of the MP2 (Table 2) and experimental rotational constants (Table 3) reveal they deviate by less than 1% in each case. There is also excellent agreement between the MP2 and experimental Δ_J and Δ_{JK} centrifugal distortion constants.

Vibrationally Excited State of *sp*. The uncorrected MP2 calculations of the vibrational frequencies (not tabulated herein) predict that there are three low-frequency fundamental modes at 171 cm^{−1} (lowest bending vibration), 213 cm^{−1} (C–C–S–H torsion), and 285 cm^{−1} (second lowest bending). The next fundamental has a frequency of 504 cm^{−1} and needs no further consideration because rotational transitions belonging to this mode would be exceedingly weak.

The ^a*R*-spectrum of one excited-state was assigned in the same manner as the ground-state spectrum. No definite assignments could be made for the *K*₁ = 1 lines and the *A* rotational constant therefore becomes very uncertain. It was noted that any reasonable value of this constant produced only a slight increase (Table 3) in the absolute value of the pseudoinertial defect defined by $\Delta = I_c - I_b - I_a$; where *I*_a, *I*_b, and *I*_c are the principal moments of inertia, from the value of Δ obtained for the ground state. A low-frequency bending vibration involving the heavy atoms would produce a sizable decrease in the absolute value of Δ , as compared to its ground-state value, whereas a torsion about the C–S bond would lead to a slight increase in Δ .³¹ The latter was observed, and it is therefore concluded that we had assigned the first excited-state of the torsion.

The *A* rotational constant was fixed at 30109 MHz in the least-squares fit, because the B3LYP vibration–rotation interaction constant α_A given by $\alpha_A = A_0 - A_1$,²⁷ where *A*₀ is the

TABLE 4: Spectroscopic Constants^a of the Ground Vibrational State of the *ac* Conformer of H₂C=C=CHSH

<i>A</i> /MHz	29256.99 (10)
<i>B</i> /MHz	2841.0484 (59)
<i>C</i> /MHz	2653.0051 (55)
Δ_J /kHz	1.182 (17)
Δ_{JK} /kHz	−66.64 (11)
Δ_K /kHz	1459 (22)
δ_J /kHz	0.20621 (54)
δ_K /kHz	9.44 (29)
number of transitions	57
rms ^b /MHz	0.145

^a Key: *A*, reduction, *I*^r, representation.²⁶ Uncertainties represent one standard deviation. ^b Root-mean-square deviation.

ground-state rotational constants and *A*₁ is the rotational constants of the first excited torsional state, was calculated to be −28.05 MHz. The spectroscopic constants of this excited-state are shown in Table 3, and the spectrum is found in the Supporting Information, Table 4S. Rough relative intensity measurements yielded *ca.* 210 cm^{−1} for this mode.

The two remaining vibration–rotation interaction constants of this state, namely α_B , and α_C , were predicted to be −0.40 and −2.14 MHz in the B3LYP calculations. These values are in order-of-magnitude agreement with their experimental counterparts (−1.85, and −3.54 MHz, respectively), which have been derived from the entries in Table 3.

Assignment of the *ac* Conformer. The largest dipole moment of this component is $\mu_b \approx 3.2 \times 10^{-30}$ C m (Table 2) and searches for the strong *b*-type *Q*-branch *K*_{−*J*} = 2 ← 1 series of transitions predicted using the spectroscopic constants in Table 2 were therefore performed. This series of lines were found close to their predicted frequencies. The ^b*R*-branch lines of the comparatively strong *K*_{−*J*} = 1 ← 0 and 2 ← 1 series were searched for next and readily assigned. The frequencies of the weak ($\mu_a \approx 2.4 \times 10^{-30}$ C m; Table 2) ^a*R*-coalescing *K*_{−*J*}-pairs of transitions could now be predicted accurately and were readily assigned.

There are two mirror-image forms of *ac* and tunneling between them should result in small splittings of the *a*- and *b*-type lines. However, no such splittings were observed, which means that they are less than the resolution power of our spectrometer, which is approximately 0.5 MHz. The absence of resolved splittings seems likely, because the barrier at the *antiperiplanar* position is predicted to be relatively high (2.97 kJ/mol; Figure 1). However, significantly larger splittings were expected for the *c*-type transitions because they should occur between vibrational levels of opposite parity. It is expected that these splittings will amount to several MHz, because of the said barrier height. Searches for these *c*-type lines were not successful, presumably because μ_c is small ($\mu_c \approx 1.5 \times 10^{-30}$ C m; Table 2).

The uncorrected MP2 values for the three lowest fundamentals were 142, 176, and 312 cm^{−1}, respectively. However, assignments were not made for any of the corresponding vibrationally excited states, presumably because of lack of intensity.

A total of 57 *a*- and *b*-type transitions were identified for the ground vibrational state of *ac* and they are listed in the Supporting Information; Table 5S, while the spectroscopic constants are displayed in Table 4. Comparison of the MP2 spectroscopic constants in Table 2 with their experimental counterparts (Table 4) reveals excellent agreement, with the exception of δ_K .

Energy Difference. The internal energy difference between conformers *ap* and *sp* has been derived using a variant of eq 3

of Esbitt and Wilson.³² According to Wilson,³³ the internal energy difference is given by

$$E_v - E'_{v'} = E'_{J'} - E_J + RT \ln L \quad (1)$$

where E_v and $E'_{v'}$ are the internal energies of the two conformers in the v and v' vibrational states, respectively, $E'_{J'}$ and E_J are the lowest energy levels of the two rotational transitions under investigation, R is the universal gas constant and T is the absolute temperature. L is given by

$$L = \frac{S' g'' (v'' \mu'')^2 l'' \Delta v' \lambda'' (2J' + 1)}{S'' g' (v' \mu')^2 l' \Delta v'' \lambda' (2J'' + 1)} \quad (2)$$

where S is the peak signal amplitude of the radiation-unsaturated line, g is the degeneracy other than the rotational degeneracy, which is $2J + 1$. v is the frequency of the transition, μ is the principal-axis dipole moment component, l is the radiation wavelength in the Stark cell,³⁴ Δv is the line breadth at half-height, λ is the line strength, and J is the principal rotational quantum number.

The internal energy difference between the ground vibrational states of conformers **ac** and **sp** was determined by comparing the intensities of several selected lines. The dipole moment is not known for the two rotamers and the values listed in Table 2 were used. The weights were assumed to be 1 for **sp** and 2 for **ac**. The **sp** conformer was found to be 1.0(6) kJ/mol more stable than **ac**, where the uncertainty of ± 0.6 kJ/mol has been estimated by taking the many sources of error of the parameters of eq 2 into consideration. The experimental value of 1.0(6) kJ/mol is close to the corrected MP2 value of 1.5 kJ/mol (Table 2). Interestingly, the B3LYP value is 1.1 kJ/mol (Table 2S; Supporting Information).

Structures

It is not possible to determine the full experimental structures of **sp** and **ac**, because only one isotopologue has been studied. It has been stated above that the experimental rotational constants differ very little from those obtained from the MP2 structures. It is interesting to compare the approximate equilibrium structures of **sp** and **ac** in Table 1 with the r_0 -structure of allene ($\text{H}_2\text{C}=\text{C}=\text{CH}_2$).³⁵ The C=C bonds in allene are 130.8(3) pm,³⁵ which is very similar to the MP2 structures (Table 1). There is also good agreement for the C–H bond lengths, which is 108.7(13) pm in allene. The MP2 calculations have been performed using a comparatively large basis set, aug-cc-pVTZ, and it has been shown³⁶ that structures derived this way are close to the equilibrium structures, which is therefore assumed to be the case for the two conformers of the title compound.

Moreover, the value of the pseudoinertial defect ($\Delta = -3.368(3) \times 10^{-20} \text{ m}^2 \text{ u}$; Table 3) of **sp** corroborates that this conformer has an exact symmetry plane, because this value is close to its counterparts (same units and magnitude) in $\text{FHC}=\text{C}=\text{CH}_2$ (-3.30),³⁷ $^{35}\text{CIHC}=\text{C}=\text{CH}_2$ (-3.26),³⁸ $^{37}\text{CIHC}=\text{C}=\text{CH}_2$ (-3.26),³⁸ $^{79}\text{BrHC}=\text{C}=\text{CH}_2$ (-3.24),³⁹ $^{81}\text{BrHC}=\text{C}=\text{CH}_2$ (-3.24),³⁹ $\text{IHC}=\text{C}=\text{CH}_2$ (-3.21),³⁸ $\text{F}_2\text{C}=\text{C}=\text{CH}_2$ (-3.20),⁴⁰ and $(\text{N}\equiv\text{C})\text{HC}=\text{C}=\text{CH}_2$ (-3.17),⁴¹ all of which have been demonstrated to have exact C_s symmetry.

The value of the C–C–S–H dihedral angle of **ac** is of special interest. The MP2 calculations above yield 140° for this angle, whereas the B3LYP value is 143° (Table 1S). This angle is very sensitive to the pseudoinertial defect. It is seen from Table 2 that the absolute value of Δ increases by $1.34 \times 10^{-20} \text{ m}^2 \text{ u}$ upon going from **sp** to **ac**. The experimental counterpart obtained from Tables 3 and 4 is 1.31 (same units). This close

agreement is taken as evidence that the C–C–S–H dihedral angle is indeed close to 140° . A liberal uncertainty limit of $\pm 5^\circ$ has been assigned to this value, which is therefore taken to be $140(5)^\circ$.

Discussion

The structural and conformational properties of $\text{H}_2\text{C}=\text{C}=\text{CHSH}$ are both similar and different from those of $\text{H}_2\text{C}=\text{CHSH}$.^{1,2} The *synperiplanar* conformers are global energy minima of both compounds. The energy differences between this form and the second rotamer is also similar, 1.0(6) kJ/mol (allenethiol) vs 0.6(3) kJ/mol for $\text{H}_2\text{C}=\text{CHSH}$.^{1,2} However, the less stable *anticlinal* form of the title compound has a C–C–S–H dihedral angle of $140(5)^\circ$ from *synperiplanar*, whereas this angle is effectively 40° larger in $\text{H}_2\text{C}=\text{CHSH}$. Allenethiol has a MP2 barrier maximum calculated to be about 3 kJ/mol at the *antiperiplanar* conformation, whereas the barrier maximum is below the energy of the ground vibrational state of $\text{H}_2\text{C}=\text{CHSH}$.^{1,2}

There is no obvious explanation for the different conformational behavior observed for the high-energy forms of ethenethiol and allenethiol. However, an interesting parallel exists for the $\text{H}_2\text{C}=\text{CHSC}\equiv\text{N}$ and $\text{H}_2\text{C}=\text{C}=\text{CHSC}\equiv\text{N}$ pair of compounds. Two rotamers have been identified for $\text{H}_2\text{C}=\text{CHSC}\equiv\text{N}$.^{42,43} The preferred form of this compound has a *synperiplanar* conformation, which is 3–6 kJ/mol more stable than the second *anticlinal* form, where the C–C–S–C dihedral angle is about 130° .^{42,43} This contrasts the findings for $\text{H}_2\text{C}=\text{C}=\text{CHSC}\equiv\text{N}$.¹⁷ The MW spectrum of only the *anticlinal* conformer, with a C–C–S–C dihedral angle of 134° , was assigned for this compound, and the quantum chemical calculations indicate that this is the global minimum of $\text{H}_2\text{C}=\text{C}=\text{CHSC}\equiv\text{N}$. It is therefore concluded that the conformational behavior of ethenethiol derivatives, substituted at the sulfur atom, can be quite different from the allenethiol derivatives, even with the same substituent.

Acknowledgment. We thank Anne Horn for her skilful assistance. The Research Council of Norway (Program for Supercomputing) is thanked for a grant of computer time. J.-C. G. thanks “Physique et Chimie du Milieu Interstellaire” (PCMI) and the “Programme National de Planétologie” (PNP) (INSU-CNRS) for financial supports.

Supporting Information Available: B3LYP results and the MW and NMR spectra. This material is available free of charge via the Internet at <http://pubs.acs.org>.

References and Notes

- (1) Tanimoto, M.; Almond, V.; Charles, S. W.; Macdonald, J. N.; Owen, N. L. *J. Mol. Spectrosc.* **1979**, *78*, 95.
- (2) Tanimoto, M.; Macdonald, J. N. *J. Mol. Spectrosc.* **1979**, *78*, 106.
- (3) Marstokk, K. M.; Møllendal, H.; Samdal, S.; Steinborn, D. *J. Mol. Struct.* **2001**, *567–568*, 41.
- (4) Strenalyuk, T.; Samdal, S.; Møllendal, H.; Guillemin, J.-C. *Organometallics* **2006**, *25*, 2090.
- (5) Lassalle, L.; Janati, T.; Guillemin, J.-C. *J. Chem. Soc., Chem. Comm.* **1995**, 699.
- (6) Hakiki, A.; Ripoll, J. L.; Thuillier, A. *Tetrahedron Lett.* **1984**, *25*, 3459.
- (7) Guillemin, J. C.; Savignac, P.; Denis, J. M. *Inorg. Chem.* **1991**, *30*, 2170.
- (8) Lassalle, L.; Legoupy, S.; Guillemin, J.-C. *Inorg. Chem.* **1995**, *34*, 5694.
- (9) Lassalle, L.; Legoupy, S.; Guillemin, J.-C. *Organometallics* **1996**, *15*, 3466.
- (10) Hakiki, A.; Ripoll, J. L.; Thuillier, A. *Bull. Soc. Chim. Fr.* **1985**, 911.

- (11) Guillemin, J.-C.; Bajor, G.; Riague, E. H.; Khater, B.; Veszprémi, T. *Organometallics* **2007**, *26*, 2507.
- (12) Møllendal, H.; Demaison, J.; Petitprez, D.; Włodarczak, G.; Guillemin, J.-C. *J. Phys. Chem. A* **2005**, *109*, 115.
- (13) Cole, G. C.; Møllendal, H.; Guillemin, J.-C. *J. Phys. Chem. A* **2006**, *110*, 9370.
- (14) Cole, G. C.; Møllendal, H.; Khater, B.; Guillemin, J.-C. *J. Phys. Chem. A* **2007**, *111*, 1259.
- (15) Mokso, R.; Møllendal, H.; Guillemin, J.-C. *J. Phys. Chem. A* **2008**, *112*, 4601.
- (16) Møllendal, H. *J. Phys. Chem. A* **2008**, *112*, 7481.
- (17) Møllendal, H.; Cole, G. C.; Guillemin, J.-C. *J. Phys. Chem. A* **2007**, *111*, 2542.
- (18) Møllendal, H.; Leonov, A.; de Meijere, A. *J. Phys. Chem. A* **2005**, *109*, 6344.
- (19) Møllendal, H.; Cole, G. C.; Guillemin, J.-C. *J. Phys. Chem. A* **2006**, *110*, 921.
- (20) Wodarczyk, F. J.; Wilson, E. B., Jr. *J. Mol. Spectrosc.* **1971**, *37*, 445.
- (21) Frisch, M. J.; Trucks, G. W.; Schlegel, H. B.; Scuseria, G. E.; Robb, M. A.; Cheeseman, J. R.; Montgomery, J. A., Jr.; Vreven, T.; Kudin, K. N.; Burant, J. C.; Millam, J. M.; Iyengar, S. S.; Tomasi, J.; Barone, V.; Mennucci, B.; Cossi, M.; Scalmani, G.; Rega, N.; Petersson, G. A.; Nakatsuji, H.; Hada, M.; Ehara, M.; Toyota, K.; Fukuda, R.; Hasegawa, J.; Ishida, M.; Nakajima, T.; Honda, Y.; Kitao, O.; Nakai, H.; Klene, M.; Li, X.; Knox, J. E.; Hratchian, H. P.; Cross, J. B.; Adamo, C.; Jaramillo, J.; Gomperts, R.; Stratmann, R. E.; Yazyev, O.; Austin, A. J.; Cammi, R.; Pomelli, C.; Ochterski, J. W.; Ayala, P. Y.; Morokuma, K.; Voth, G. A.; Salvador, P.; Dannenberg, J. J.; Zakrzewski, V. G.; Dapprich, S.; Daniels, A. D.; Strain, M. C.; Farkas, O.; Malick, D. K.; Rabuck, A. D.; Raghavachari, K.; Foresman, J. B.; Ortiz, J. V.; Cui, Q.; Baboul, A. G.; Clifford, S.; Cioslowski, J.; Stefanov, B. B.; Liu, G.; Liashenko, A.; Piskorz, P.; Komaromi, I.; Martin, R. L.; Fox, D. J.; Keith, T.; Al-Laham, M. A.; Peng, C. Y.; Nanayakkara, A.; Challacombe, M.; Gill, P. M. W.; Johnson, B.; Chen, W.; Wong, M. W.; Gonzalez, C.; Pople, J. A. *Gaussian 03, revision B.03*; Gaussian, Inc.: Pittsburgh PA, 2003.
- (22) Møller, C.; Plesset, M. S. *Phys. Rev.* **1934**, *46*, 618.
- (23) Becke, A. D. *Phys. Rev. A* **1988**, *38*, 3098.
- (24) Lee, C.; Yang, W.; Parr, R. G. *Phys. Rev. B* **1988**, *37*, 785.
- (25) Peterson, K. A.; Dunning, T. H., Jr. *J. Chem. Phys.* **2002**, *117*, 10548.
- (26) Watson, J. K. G. *Vibrational Spectra and Structure*; Elsevier: Amsterdam, 1977; Vol. 6.
- (27) Gordy, W.; Cook, R. L. *Microwave Molecular Spectra*. In *Techniques of Chemistry*; John Wiley & Sons: New York, 1984; Vol. XVII.
- (28) McKean, D. C.; Craig, N. C.; Law, M. M. *J. Phys. Chem. A* **2008**, *112*, 6760.
- (29) Ray, B. S. *Z. Phys.* **1932**, *78*, 74.
- (30) Sørensen, G. O. *J. Mol. Spectrosc.* **1967**, *22*, 325.
- (31) Hanyu, Y.; Britt, C. O.; Boggs, J. E. *J. Chem. Phys.* **1966**, *45*, 4725.
- (32) Esbitt, A. S.; Wilson, E. B. *Rev. Sci. Instrum.* **1963**, *34*, 901.
- (33) Wilson, E. B. Personal communication.
- (34) Townes, C. H.; Schawlow, A. L. *Microwave Spectroscopy*; McGraw-Hill: New York, 1955.
- (35) Hirota, E.; Matsumura, C. *J. Chem. Phys.* **1973**, *59*, 3038.
- (36) Helgaker, T.; Gauss, J.; Jørgensen, P.; Olsen, J. *J. Chem. Phys.* **1997**, *106*, 6430.
- (37) Ogata, T.; Fujii, K.; Yoshikawa, M.; Hirota, F. *J. Am. Chem. Soc.* **1987**, *109*, 7639.
- (38) Ogata, T.; Niide, Y. *J. Chem. Soc., Faraday Trans.* **1996**, *92*, 4889.
- (39) Ogata, T.; Niide, Y. *J. Chem. Soc., Faraday Trans.* **1992**, *88*, 3517.
- (40) Durig, J. R.; Li, Y. S.; Tong, C. C.; Zens, A. P.; Ellis, P. D. *J. Am. Chem. Soc.* **1974**, *96*, 3805.
- (41) Bouchy, A.; Demaison, J.; Roussy, G.; Barriol, J. *J. Mol. Struct.* **1973**, *18*, 211.
- (42) Beukes, J. A.; Klæboe, P.; Møllendal, H.; Nielsen, C. J. *J. Mol. Struct.* **1995**, *349*, 37.
- (43) Beukes, J. A.; Klæboe, P.; Møllendal, H.; Nielsen, C. J. *J. Raman Spectrosc.* **1995**, *26*, 799.

JP901817M